
Molecular Crystals and Liquid Crystals Science and Technology. Section A. Molecular Crystals and Liquid Crystals

Publication details, including instructions for authors and subscription information:
http://www.tandfonline.com/loi/gmcl19

# An Electrooptic Effect from Liquid Crystal Monolayers

Gerd Forstmann [a], Tim Herod [b], Jie Wu [b], Randolph Duran [b] & Diethelm Johannsmann [a]

[a] Max-Planck-Institute for Polymer Research, P.O. Box 3148, D-55021, Mainz, Germany

[b] Department of Chemistry, University of Florida, Gainesville, FL, 32611-7200, USA

Version of record first published: 24 Sep 2006

To cite this article: Gerd Forstmann, Tim Herod, Jie Wu, Randolph Duran & Diethelm Johannsmann (2000): An Electrooptic Effect from Liquid Crystal Monolayers, Molecular Crystals and Liquid Crystals Science and Technology. Section A. Molecular Crystals and Liquid Crystals, 350:1, 29-41

To link to this article: http://dx.doi.org/10.1080/10587250008025230

*Mol. Cryst. Liq. Cryst.*, Vol. 350, pp. 29-41
Reprints available directly from the publisher
Photocopying permitted by license only





# An Electrooptic Effect from Liquid Crystal Monolayers

GERD FORSTMANN[a], TIM HEROD[b], JIE WU[b], RANDOLPH DURAN[b] and DIETHELM JOHANNSMANN[a*]

*[a]Max-Planck-Institute for Polymer Research, P.O. Box 3148, D-55021 Mainz, Germany and [b]Department of Chemistry, University of Florida, Gainesville, FL 32611-7200, USA*

*(Received March 25, 1999; In final form September 21, 1999)*

We report on electrooptic measurements on Langmuir-Blodgett (LB) monolayers of a 1/1 mixture of n-octyl-cyanobiphenyl (8CB) and stearic acid. The required sensitivity is achieved by depositing the LB-film on a thin gold layer and measuring the field-induced shift of the surface plasmon resonance. The existence of a finite electrooptic coefficient is proof of polar anisotropy in the monolayer. The electrooptic coefficient depends on details of the deposition process and does not change with temperature or frequency of the applied electric field.

*Keywords:* liquid crystals; LB-films; electro-optic coefficient; Pockels-effect; surface orientational anchoring

## INTRODUCTION

The structure of molecular monolayers adsorbed to solid surfaces plays an important role in many fields of surface physics such as adhesion, tribology, catalysis, or biophysics. For liquid crystal (LC) monolayers the orientation is of particular interest, because the orientation of LC monolayers should be correlated with the orientation of a bulk nematic phase in contact with an identical surface. This correlation is of high interest in the context of surface-induced alignment of nematic liquid crystals.[1,2] The details of this surface-LC interaction are largely unknown.

* Author for correspondence Phone: 49-6131-379 163 Fax: 49-6131-379 360 e-mail: johannsmann@mpip-mainz.mpg.de

To date there is no experimental technique to determine the whole orientation distribution function of a monomolecular layer. Only certain weighted averages or "moments" may be derived. Second moments like $\langle\cos^2\theta\rangle$ can be determined with linear optical spectroscopy and linear dichroism in particular.[3,4] Odd moments, on the other hand, are not accessible with linear optics. For example, it cannot be determined from IR-dichroism whether the dipole moment of a polar moiety points towards the surface or away from it. Odd moments like $\langle\cos^3\theta\rangle$ are, however, accessible with nonlinear optical techniques.[5,6,7]. Using optical second harmonic generation (SHG), Shen and co-workers proved that cyanobiphenyls exhibit polar anisotropy when adsorbed on sufficiently polar surfaces.[8] This contrasts with the bulk nematic phase where the orientation distribution function has quadrupolar symmetry.[9] Apparently, the molecule–substrate interaction is strong enough to overcome the tendency to form quadrupolar pairs.[10]

In the case of SHG, monolayer sensitivity is readily achieved because the technique has little background and photon-counting can be employed.[11] For electrooptic measurements, sensitivity is a more critical issue. In this work, we show that the Pockels effect of an LC monolayer is measurable in an optically resonant configuration. The layer is deposited on a thin gold film and the field-induced shift of the surface plasmon polariton ("plasmon" for short) is used to probe the electrooptic effect.[12] This technique has been used in the past to measure the Pockels effect on polymeric waveguides.[13] The magnitude of the electrooptic coefficient is an indicator of polar anisotropy in the layer.

The measurements discussed here are attractive because they are rather simple, especially with regard to instrumentation. They can be performed on any optical reflectometer without the need for high power lasers like in SHG. Potentially, they could be performed with discharge lamps instead of lasers, which would make a spectroscopic extension straightforward. Finally, optically detected monolayer dielectric spectroscopy seems feasible by sweeping the frequency of the electric field.

## SAMPLE PREPARATION

We investigated 1/1 mixtures of n-octyl-cyanobiphenyl (8CB) and stearic acid (SA). Fig. 1 shows the chemical structure. The electrooptic activity mainly originates from the 8CB molecules which contain an asymmetric $\pi$-electron system. 8CB has been used as a model compound in many liquid crystal investigations. It has a permanent dipole moment of 5 Debye[14] and forms stable monolayers on the water surface.[15] However, transfer of these monolayers onto solid substrates is difficult. This difficulty can be avoided by using a mixture of 8CB and stearic

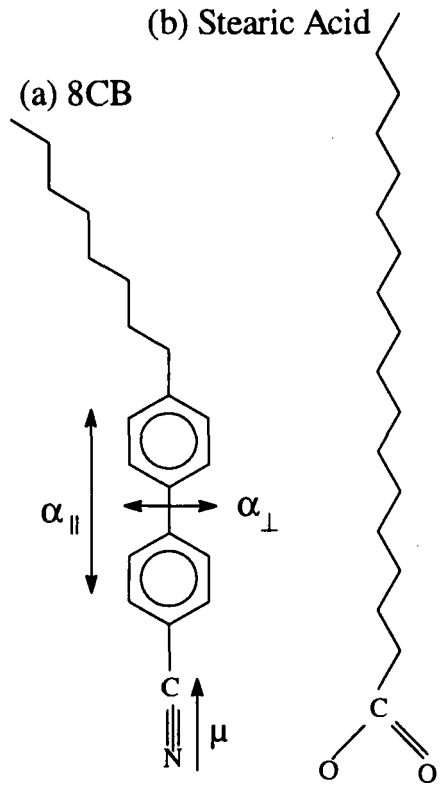


FIGURE 1 Chemical structure of the substances used. 8CB has a permanent molecular dipole μ of about 5 Debye. It exhibits an anisotropic polarizability ($\alpha_{\parallel}>\alpha_{\perp}$) and a non-vanishing hyperpolarizability β. 8CB was mixed with stearic acid (b) to obtain stable monolayers

acid, rather than pure 8CB.[16] Fig. 2 shows the π-A diagram and indicates the different transfer pressures investigated in this study. The π-A diagram exhibits an extended plateau at about 9 mN/m. Enderle and co-workers concluded from SHG measurements that the plateau is caused by a coexistence of a monolayer and a multilayer. As the area is decreased, 8CB is squeezed out from the bottom layer to form patches with quadrupolar order ontop of the first layer.[16] Below 9 mN/m, the π-A diagram shows a straight and featureless increase of pressure which is indicative of a homogeneously mixed monolayer. This picture is corroborated by Brewster angle micrographs which do not show any structure below 9 mN/m.

The substrates were prepared by evaporating a 0.8 nm chromium layer and a 47 nm gold layer onto BK7 glass slides. The evaporation rates were 0.5 nm/s for the bulk gold and 0.05 nm/s for the first and last 3 nm. The substrates were stored

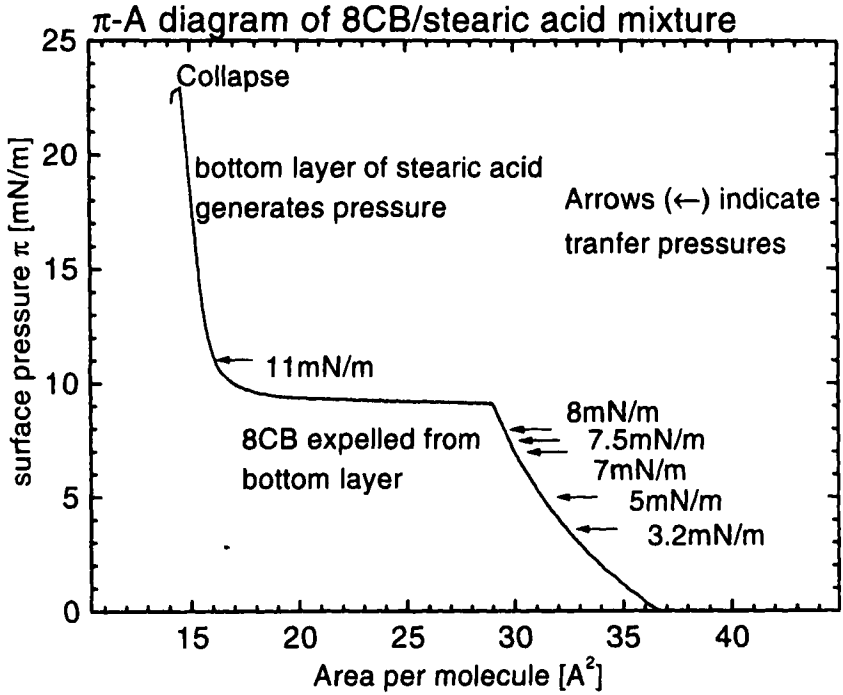


FIGURE 2 π-A diagram of a 1/1 mixture of 8CB and stearic acid. Below a pressure of 9 mN/m one finds a homogeneously mixed phase

in methanol after evaporation and treated with an argon-oxygen plasma prior to LB-transfer. A KSV-1000 trough was used for LB-deposition. 250 μl of a $10^{-3}$ M solution were spread on MilliQ-water after immersion of the sample. After compression the monolayer was transferred at an upstroke speed of 3 mm/min and various applied surface pressures. The transfer ratio was between 0.9 and 1. The coated samples were assembled to cells with Mylar spacers (Goodfellow) with a nominal thickness of 6 μm. According to the static reflectivity measurements (Fig. 4) the air gaps obtained after cell assembly were between 7 and 10 μm wide.

## EXPERIMENTAL PROCEDURE AND DATA ANALYSIS

Fig. 3 shows a sketch of the experimental setup. The sample is mounted in the Kretschmann configuration to excite a surface plasmon[17] which results in a sharp

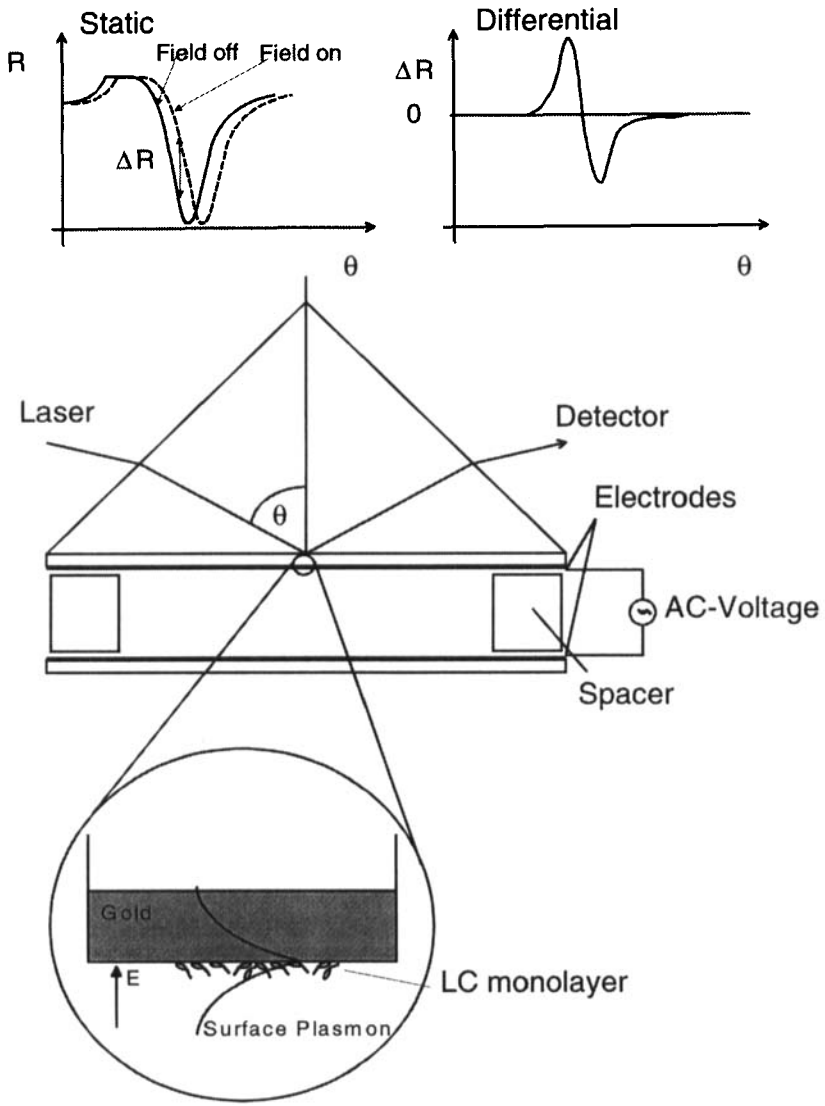


FIGURE 3 Experimental setup

dip of the reflectivity $R(\theta)$ at the angle of incidence fulfilling the coupling condition. It is well known that the optical thickness of dielectric films on metal surfaces can be determined with submonolayer accuracy from the shift of the surface plasmon coupling angle.[17] The angle resolution of the goniometer is 0.01° which corresponds to a thickness resolution of about 0.1 Å. Small changes

of the coupling angle caused by an external stimulus (such as an electric field) are detected with even greater sensitivity by referencing the lock-in amplifier to the modulated external stimulus.[13] After proper electrical shielding and averaging, changes in reflectivity are well measurable down to the level of $\Delta R \sim 10^{-6}$. With this sensitivity, the Pockels effect of samples as thin as even a monolayer becomes measurable.

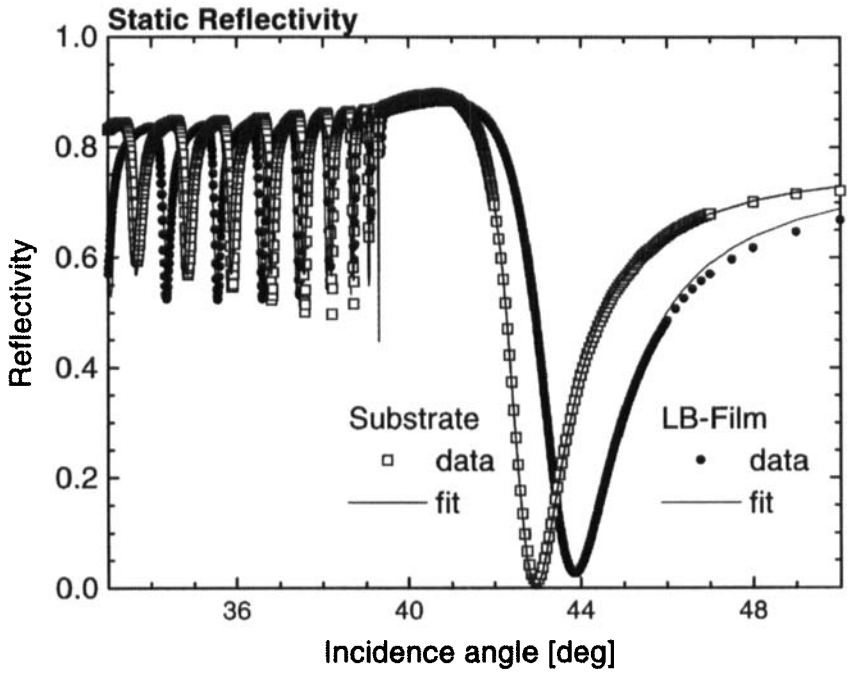


FIGURE 4 Static reflectivities $R(\theta)$ for a bare gold surface and the same gold surface covered with an LB-layer and assembled to a cell (p-polarization). The straight line is the Fresnel calculation. The broad minimum corresponds to the surface plasmon. From the position of the plasmon minimum the thickness of the LB-layer is derived. The minima below the critical angle are Fabry-Perot resonances. The surface plasmon is unaffected by the second electrode. From the spacing of the Fabry-Perot resonances the gap width $d$ is derived

The static reflectivity as a function of incidence angle $R(\theta)$ is measured before and after each EO measurement (Fig. 4). From the position of the coupling angle the thickness of the deposited film is determined. The width of the air gap between the film of interest and the counter electrode is derived from the coupling angles of the Fabry-Perot resonances below the critical angle. Around the plasmon coupling angle $R(\theta)$ is not affected by the counter electrode because the

decay length of optical field (~ 0.1 μm) is much less than the width of the air gap (~ 7 μm).

For the EO measurements, a signal generator (HP3325A) and a home-built amplifier were used to apply an oscillating voltage of $U_{peak} = \pm 130$ V across the gap. With a gap width of 10 μm this amounts to a field strength of the order of $10^7$ V/m. The change in reflectivity $\Delta R(\theta)$ is detected with a photodiode and a lock-in amplifier (EG&G5302), the latter being referenced to the AC-voltage. Electronic cross-talk between the sample and the detector is significant for frequencies larger than 10 kHz. At these frequencies, an offset (determined with the laser turned off) is subtracted from the data. Both the real ("$x$") and the imaginary ("$y$") component of the signal are recorded. There is a phase shift of electronic origin between the function generator output and the detector output. In order to correct for this phase the signal is rotated numerically in the complex plane by a constant phase angle $\varphi_0$, such that the "$y$"-component is minimized. After minimization, the rotated "$x$"-component ($\sim\Delta R$) is larger than the "$y$"-component by at least a factor of 10. The sign of $\Delta R$ is determined from its low frequency values where the phase angle $\varphi_0$ is small.

Calibration of $\Delta R$ was done with a light chopper. The frequency dependence of the detector response was determined by replacing the sample with a Pockels cell, where the response of the Pockels cell was assumed to be independent of frequency $f$. The amplifier output $U(f)$ was measured by directly inputting it to the lock-in amplifier. The width of the air gap $d$ is known from the Fabry-Perot fringes in the static reflectivity. The electric field $E(f)$ is then given as $U(f)/d$.

Special care was taken to eliminate acoustic artifacts. Acoustic effects are clearly evidenced by an audible sound at twice the exciting frequency. It originates from electrostatic attraction between the electrodes. Due to small asymmetries in the mounting structure the movement of the sample plate contains a small rotatory components. Since the setup is extremely sensitive to oscillatory rotations of the sample, they result in an artifact in the $\Delta R(\theta)$ curve at the second harmonic frequency. The second harmonic signal is largely irreproducible. As a consequence, the EO Kerr effect cannot be measured in this configuration.

The signal at the fundamental frequency is unaffected by these acoustic artifacts. An acoustic artifact at the fundamental could, in principle, occur if there was a spurious DC bias voltage across the electrodes. The overall electrostatic attraction between the plates would then contain a component at the fundamental frequency. We therefore deliberately added a DC bias voltage to the amplifier output and measured $\Delta R$ as a function of bias voltage. If the observed signal was of acoustic origin, one could compensate the spurious bias voltage giving rise to the artifact. As Fig. 5 shows, this is not the case. The signal never vanishes and is smallest with no added bias voltage. We conclude that the signal obtained with-

out a bias voltage is indeed caused by the Pockels effect. Further support to this conclusion is given by the shape of $\Delta R(\theta)$. While the acoustic artifact should result in a purely antisymmetric curve, the experimental data contain a symmetric contribution.

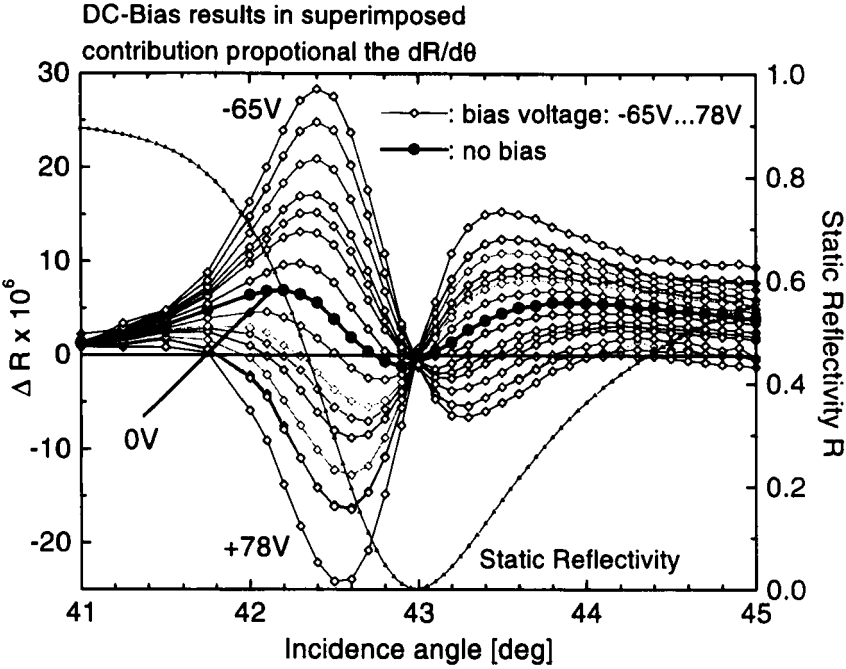


FIGURE 5 $\Delta R(\theta)$ signals, where an acoustic artifact has deliberately been introduced by applying a DC bias voltage across the gap. In this case the electrostatic attraction caused by the modulation of the electric field contains a 1f-component, which is clearly evidenced in the data. At no point does the DC-bias voltage compensate the EO-effect, proving that the EO-effect itself is not an acoustic artifact

EO modeling proceeds according to the Fresnel equations. Table I gives the optical parameters. Because reference experiments on bare gold show an EO effect even for the uncovered substrate, the model includes two separate EO-active layers: a thin surface layer of gold with a thickness of about the Thomas-Fermi screening length and the 8CB/SA film. The dielectric constant of EO-active layers changes under the influence of the electric field by $\Delta\varepsilon = -\varepsilon^2 r E = -\varepsilon^2 (r' + ir'') E$, with $r = d(1/\varepsilon) / dE$the electrooptic coefficient.[18] Since the polarization of the surface plasmon is close to vertical,[19] the experimentally determined $r$-coefficient is close to the $r_{33}$-component of the EO tensor.

TABLE I Optical parameters used for modeling

| *Layer* | *Thickness [nm]* | *Dielectric permittivity* ε |
|---|---|---|
| BK7 glass slide | ∞ | 2.296 |
| Chromium | 0.8 | − 3.12 + i 18.0 |
| Gold | 47.5 | − 12.49 + i 1.30 |
| EO-active surface layer of gold | ~ 0.1 | − 12.49 + i 1.30 |
| 8CB/Stearic Acid | 3 | 2.86 + i 0.66 |
| Air Gap | 7500 | 1 |
| Counter electrode | ∞ | − 12.49 + i 1.30 |



The linear-optical input parameters to the fit are determined from the static $R(\theta)$ curves of the bare and the LB-film covered substrate. A dielectric constant of $\varepsilon_{LB} = 2.86$ was assumed for the LB-film.[14] Since $\varepsilon_{LB}$ depends on orientation the uncertainty is rather large. The film thickness is 3 ± 0.5 nm, where the error originates from the uncertainty on $\varepsilon_{LB}$. After the linear-optical parameters have been fixed, the function $\Delta R(\theta)$ contains the free parameters $r'_{MS}$, $r''_{MS}$, $r'_{LB}$, and $r''_{LB}$, where the indices MS and LB stand for the metal surface and LB-film, respectively. $r'_{MS}$and $r''_{MS}$ are determined from the experiments on bare gold. $r'_{LB}$, and $r''_{LB}$ are determined from experiments with the LB-film present, where it was assumed that the EO coefficient of the gold surface layer was unaffected by the LB-film. This assumption is further justified in the Results section. The real and the imaginary part of the EO-coefficient are well separated in the fit because a real EO coefficient induces a $\Delta R(\theta)$ curve which is largely antisymmetric around the coupling angle, while the imaginary component induces a rather symmetric curve.

## RESULTS AND DISCUSSION

Fig. 6a shows the static reflectivity and the electrooptic signal obtained at a frequency of 1 kHz on a sample transferred at a surface pressure of 8 mN/m. The electrooptic signal is not purely antisymmetric around the minimum of the surface plasmon curve which would be expected if the plasmon was only shifted along the angular scale. Apparently, the electric field also changes the shape of the plasmon such that the plasmon becomes narrower in the presence of the electric field. Interestingly, experiments on bare gold also show an EO effect as shown in Fig. 6b. We believe that the field-induced narrowing of the surface plasmon curve is caused by a shift of the band structure in the near-surface

region of the gold. This aspect will be covered in more detail in a separate publication.[20] Here, we just subtract this contribution. Before subtraction, the signal from the bare gold surface has to be shifted on the angular scale in order to account for the shift of the plasmon due to the LB-layer (arrows in Fig. 6). After the subtraction procedure, $\Delta R(\theta)$ appears largely antisymmetric, suggesting a real EO coefficient. The best fit is $r' = (1.2 \pm 0.2 - i\,0.4 \pm 0.1)$ pm/V.

Different possibilities exist for the origin of the observed electrooptic effect. Firstly, the organic layer on the gold may modify the electrooptic properties of the near-surface region of the gold. In this case the LB-film itself would be EO-inactive. To test for this possibility, we performed reference experiments with aliphatic thiols which adhere well to gold but should be EO-inactive.[20] These do indeed affect the EO activity of the gold. However, the effect has opposite sign compared to the results found for 8CB/SA. Also, the terminal sulfur groups of the thiols are believed to chemically interact with the gold, while the interaction of the 8CB with the gold should be smaller. We conclude that a modified EO activity of the gold surface can not be the only factor underlying our observations.

Secondly, the observed effects can be caused by purely electronic nonlinearities in the 8CB molecules. An order of magnitude estimation shows that this is a plausible explanation. Unfortunately, we are not aware of theoretical or experimental values of the microscopic hyperpolarizability of 8CB at $\lambda = 633$ nm, which could be used for quantitative comparison. Rasing and coworkers have determined the hyperpolarizability $\alpha_{\zeta\zeta\zeta}^{(2)}$ at $\lambda = 532$ nm with optical SHG as $2.5\ 10^{-29}$ esu.[21] However, these values are strongly influenced by resonant enhancement close to $2\omega$. Assuming that the non-resonant hyperpolarizability is ten times less that value, we find an $r$-coefficient of $r' = \langle\cos^3(\alpha)\rangle\ 3$ pm/V. Comparison with the experimental value of 1 pm/V shows that a purely electrooptic effect is well compatible with the data.

Thirdly, reorientation of molecules in the electric field might also play a role. Since 8CB is highly birefringent, reorientation will affect the refractive indices as well. This effect can only be operative on molecules which are aligned neither perfectly parallel to the surface nor perfectly perpendicular to the surface. The effect scales with $\langle\cos^2(\alpha)\sin(\alpha)\rangle$ where the angular brackets denote the ensemble average and $\alpha$ is the angle from the surface normal. From what is known about 8CB monolayers, it seems unlikely that $\langle\cos^2(\alpha)\sin(\alpha)\rangle$ should be exactly zero or even very small. 8CB is tilted on the water surface and is expected to retain some of this tilt after transfer to a solid substrate. Assuming that $\langle\cos^2(\alpha)\sin(\alpha)\rangle$ is larger than 0.01 one can derive an upper bound for the average reorientation which is about $\delta\alpha < 0.1°$. Apparently, the orienting potential at the gold surface is fairly high. As a consequence, the orientational anchor-

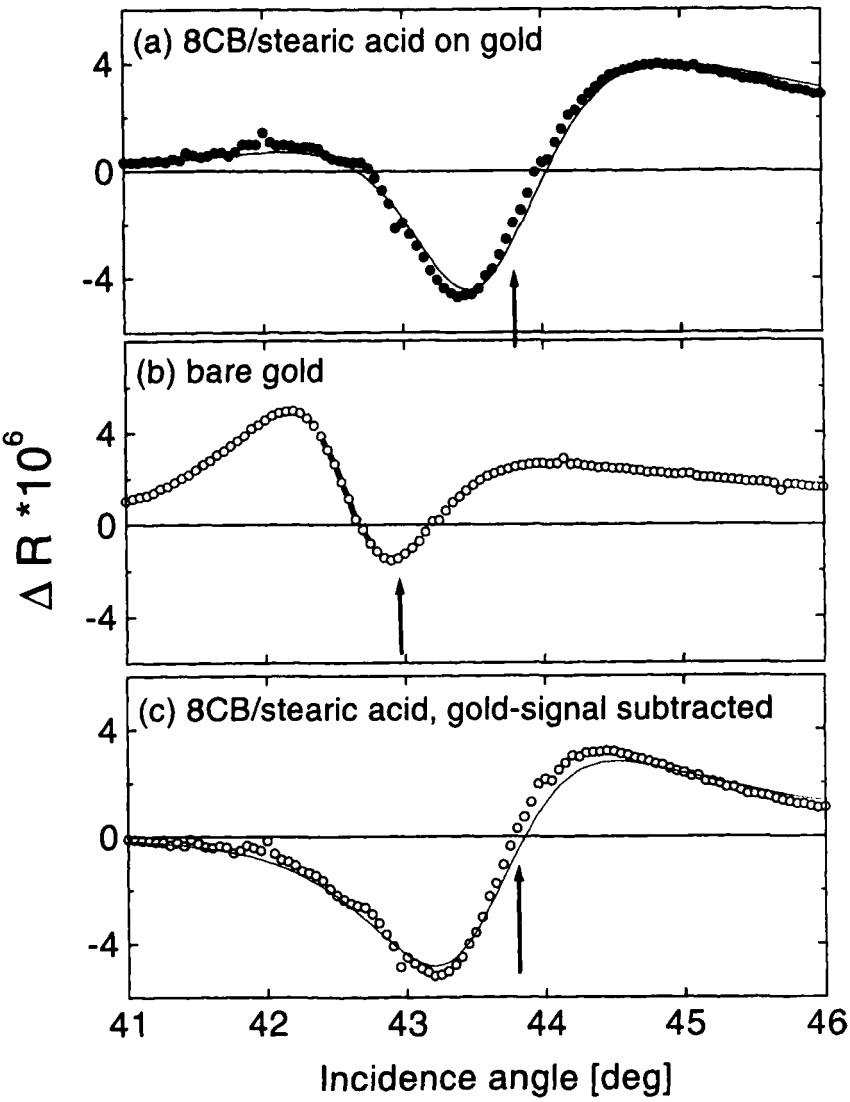


FIGURE 6 Differential reflectivities $\Delta R(\theta)$ for a sample with the LB-film present (a), the bare gold substrate (b) and the difference of the two. The arrows indicate the minima of the static reflectivity. For subtraction of the EO-signal from the bare gold, the data have been shifted on the angular scale such that the coupling angles coincide

ing energy[22] should be high, as well. In order to further investigate the question of a possible field-induced reorientation, we performed measurements at different frequencies and temperatures. A purely electronic effect should neither

depend on frequency nor on temperature. Indeed the EO-signal does not vary in the frequency range from 0.1 to 10 kHz and the temperature range from 25 to 75°C. At temperatures higher than 75°C the layer evaporates as evidenced from the shift of the static surface plasmon.

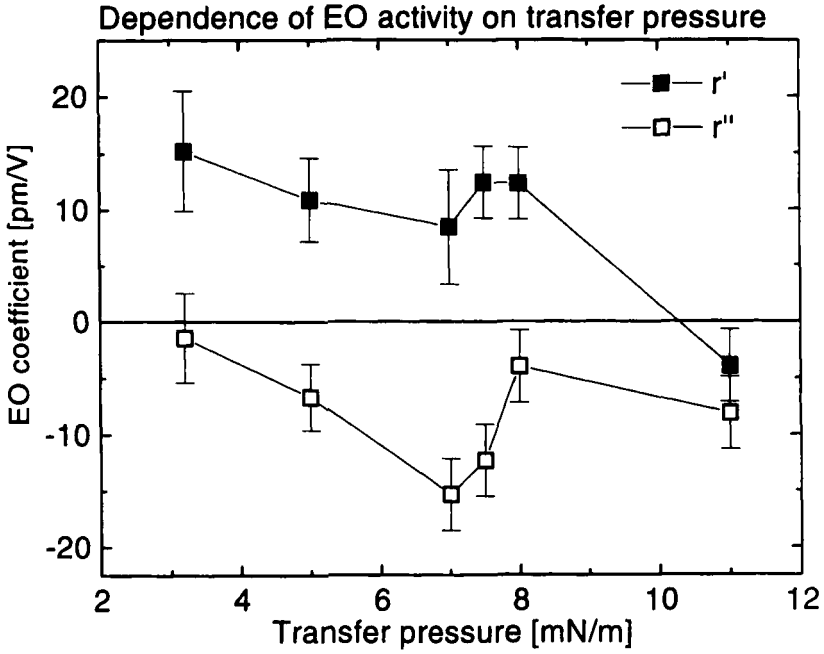


FIGURE 7 Dependence of the electrooptic coefficient of the LB-layer on the transfer pressure

Finally, we investigated the dependence of the EO signal on the transfer pressure (Fig. 7). The real part does not vary much for transfer pressures below the coexistence plateau. It is much lower and even changes sign for transfer pressures above the coexistence plateau. This finding is compatible with the model by Enderle and co-workers who claim that one has a multilayer structure above the plateau. Note that the surface coverage does not vary much for the range of transfer pressures investigated. The variation of $r''$ with coverage is somewhat surprising. The variation could be caused by a dependence of the LB-layer-substrate interaction on the transfer pressure. A second explanation would be a field-induced generation of scattering centers. Scattering broadens the plasmon in a similar way as absorption. This hypothesis would imply that field-induced molecular motion is indeed present. The generation of scattering centers is expected to depend on details of the deposition process and to attribute much significance to the detailed dependence of $r''$ on transfer pressure.

## CONCLUSIONS

We have measured the electrooptic activity of Langmuir-Blodgett monolayers of a 1/1 mixture or 8CB and stearic acid. The most plausible cause for the effect is the electronic hyperpolarizability of 8CB. Field-induced reorientation of the molecules may also contribute. From an order of magnitude estimation, we conclude that the reorientation should be less than 0.1° which points to a rather strong microscopic orientational anchoring potential.

### *Acknowledgements*

G. Herrmann, H. Bock and A. Scheller gave very valuable support for this work. Tim Herod acknowledges the support of the German Academic Exchange Service (DAAD) and the Young Investigator Award from the National Science Foundation. Jie Wu was supported through the Florida Engineering Research Center on Particle Science and Technology.



### *References*

1 J. Cognard, *Alignment of Liquid Crystals and their Mixtures*, Gordon and Breach, London 1982.
2 B. Jérôme, *Rep. Prog. Phys.* **54**, 391 (1991).
3 J. Michl, E.W. Thulstrup, *Spectroscopy with Polarized Light*, VCH Publishers, New York 1986.
4 K. Weiss, C. Wöll, E. Böhm, B. Fiebranz, G. Forstmann, B. Peng, V. Scheumann, D. Johannsmann, *Macromolecules* **31**, 1930 (1998).
5 Q. Du, E. Freysz, Y.R. Shen, *Phys. Rev. Lett.* **72**, 238 (1994).
6 M.B. Feller, W. Chen, Y.R. Shen, *Phys. Rev. A* **43**, 6778 (1991).
7 Y.-C. Chang, C.W. Frank, G.G. Forstmann, D. Johannsmann, *J. Chem. Phys.* **111**, 6136 (1999).
8 C.S. Mullin, P. Guyot-Sionnest, Y.R. Shen, *Phys. Rev. A* **39**, 3745 (1989).
9 P.-G. de Gennes, J. Prost, *The Physics of Liquid Crystals*, Oxford University Press, Oxford 1993.
10 A. de Vries, *Mol. Cryst. Liq. Cryst.* **10**, 219 (1970).
11 Y.R. Shen, Annu. *Rev. Phys. Chem.* **40**, 327 (1989).
12 J.C. Loulergue, M. Dumont, Y. Levy, *Thin Solid Films* **160**, 399 (1988).
13 V. Dentan, Y. Levy, M. Dumont, P. Robin, E. Chastaing, *Opt. Commun.* **69**, 379 (1989).
14 D.A. Dunmur, M.R. Manterfield, W.H. Miller, J.K. Dunleavy, *Mol. Cryst. Liq. Cryst.* **45**, 127 (1978).
15 J. Xue, C. Jung, M.W. Kim, *Phys Rev. Lett.* **69**, 474 (1992).
16 T. Enderle, A.J. Meixner, I. Zschokke-Granacher, *J. Chem. Phys.* **101**, 4365 (1994).
17 Knoll, W. *MRS Bulletin* **29**, (1991).
18 R.W. Boyd, *Nonlinear Optics*, Academic Press 1992.
19 For the given configuration the deviation of the polarization vector from the surface normal is 13°.
20 G.G. Forstmann, D. Johannsmann, in preparation.
21 Th. Rasing, G. Berkovic, Y.R. Shen, S.G. Grubb, M.W. Kim, *Chem. Phys. Lett.* **130**, 1 (1986).
22 H. Yokoyama, *Mol. Cryst. Liq. Cryst.* **165**, 265 (1988).